Magnetic Particles

DOI: 10.1002/anie.201001031

Magnetoresponsive Microparticles with Nanoscopic Surface Structures for Remote-Controlled Locomotion**

Shin-Hyun Kim, Jae Young Sim, Jong-Min Lim, and Seung-Man Yang**

Microparticles with photonic, magnetic, and structural functionalities have been intensively studied owing to their potential applications in biological probes, microfluidic pumps and mixers, and microdisplay devices.[1] Particularly, Janus particles have been prepared by various approaches to induce anisotropic properties on particles.[2] Recent studies on functional microparticles have focused on continuous microfluidic synthesis owing to the greater flexibility of this approach in terms of the shape and constituent materials of the synthesized microparticles. Microparticles have been generated by polymerization of photocurable droplets with simple,[3] Janus,[4] and multiple shapes[5] or designed by lithographic techniques in the course of flow within microfluidic devices with photomasks[6] and digital micromirror devices.[7] In work on magnetoresponsive microparticles, Yuet et al. prepared superparamagnetic Janus particles that could be aligned and assembled by an external magnetic field.[4e] Furthermore, Chen et al. produced spherical particles with anisotropic magnetic properties from photocurable double emulsion droplets and showed that these particles display eccentric rotational motion under an applied magnetic field.[5d] To date, however, the remote manipulation of the translational motion of microparticles in a fast, simple, and precise manner, which is of practical significance in biological applications, has yet to be achieved, although the complex technique of optomagnetic trapping has been developed.[8] Moreover, the introduction of sub-micrometer-scale structural features and chemical functionalities is a topic of intense interest in microparticle synthesis, especially for the incorporation of biomolecules. Recently, we prepared Janus microparticles composed of superhydrophobic and hydrophilic hemispherical faces with distinctively different surface structures of dimple-decorated microspheres at the water-repelling interface.[9]

Herein, we present a simple and reliable method that enables both the introduction of complex surfaces onto microparticles as well as the remote control of microparticle translational motion. In the proposed method, microparticles are synthesized using a combination of two distinct approaches: microfluidic synthesis to achieve size and shape uniformity, and colloidal self-organization to generate complex surface structures. Specifically, the colloidal suspension was emulsified in an aqueous continuous phase (Figure 1 a).

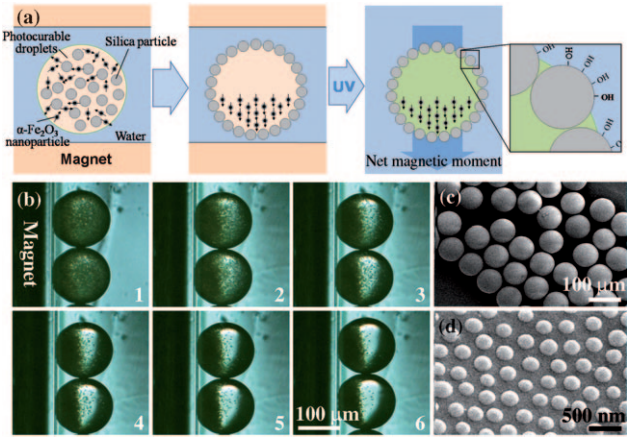

Figure 1. a) Preparation of magnetic Janus particles with net magnetic moment and surface complexity. The silica particles have silanol groups on the area exposed to the aqueous phase. b) Optical microscope (OM) images of photocurable droplets containing silica microspheres and iron oxide nanoparticles under a magnetic field of 2.78 kG. The images were taken at five-minute intervals. c, d) SEM images of magnetic Janus particles (c) and their surface (d).

The emulsion droplets consisted of the photocurable resin ethoxylated trimethylolpropane triacrylate (ETPTA) containing iron oxide nanoparticles (hematite; α-Fe_2O_3) smaller than 50 nm and monodisperse silica particles of diameter 330 nm. Because hematite nanoparticles larger than 8 nm are weakly ferromagnetic at room temperature,[10] application of a nonuniform magnetic field to the suspension induced alignment of the magnetic moment of the nanoparticles within each droplet and migration of the nanoparticles within the droplet by magnetophoresis. The silica particles within each droplet were anchored at the ETPTA–water interface to minimize the interfacial energy, and they self-organized into a two-dimensional ordered arrangement.[9,11] Therefore, by photopolymerization of ETPTA, we can create magnetic

[*] Dr. S.-H. Kim, J. Y. Sim, Dr. J.-M. Lim, Prof. S.-M. Yang
National Creative Research Initiative Center for Integrated Optofluidic Systems
and
Department of Chemical and Biomolecular Engineering
KAIST, Daejeon, 305-701 (Korea)
Fax: (+82) 42-350-5962
E-mail: dmz@kaist.ac.kr
smyang@kaist.ac.kr
Homepage: http://msfl.kaist.ac.kr

[**] This work was supported by a grant from the Creative Research Initiative Program of the Ministry of Education, Science, and Technology for "Complementary Hybridization of Optical and Fluidic Devices for Integrated Optofluidic Systems." We thank Prof. Howard A. Stone, Princeton University, for helpful discussions.

Supporting information for this article is available on the WWW under http://dx.doi.org/10.1002/anie.201001031.

Janus particles with a net magnetic moment whose surfaces are decorated with silica particle arrays.

Figure 1b shows a series of optical microscope (OM) images of photocurable droplets containing silica microspheres and iron oxide nanoparticles under a magnetic field of 2.78 kG, taken at five-minute intervals. The shift in the distribution of magnetic nanoparticles within each droplet can be discerned in the images. After 25 min, a clear boundary is observed between the magnetic nanoparticle-depleted (transparent) and nanoparticle-concentrated (opaque) hemispheres. We used a microfluidic device composed of coaxial glass capillaries to generate droplets of equal size (Figure S1 in the Supporting Information). Indeed, highly monodisperse emulsion droplets were generated at the end of the inner capillary in the dripping regime, resulting in monodisperse microparticles (Figure 1c and Figure S2 in the Supporting Information). On the other hand, the SEM images of the final microparticles show hexagonal arrays of silica particles on the microparticle surfaces (Figure 1d).

When the synthesized microparticles were placed in an external magnetic field, they aligned in such a way that the opaque hemispheres faced toward the magnetic field (Movie S1 in the Supporting Information). Figure 2a,b shows OM images of magnetic Janus particles on a planar substrate subjected to a magnetic field either parallel or perpendicular to the substrate.

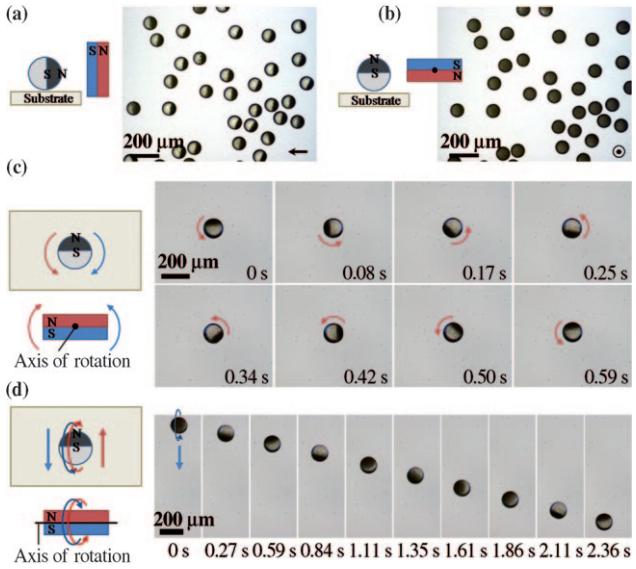

Figure 2. a,b) Alignment of magnetic Janus particles under an external magnetic field with parallel (a) and perpendicular orientations (b). c,d) Schematic illustration and OM images showing rotational motion of the magnetic particles under an external magnetic field induced by a rotating magnet with a vertical axis (c) and rotation-induced translational motion by a rotating magnet with a parallel axis (d).

By applying a rotating magnetic field, we could precisely control the rotational and translational motion of the as-prepared magnetic Janus particles. Because the opaque hemisphere orients toward the field direction, we were able to rotate the microparticles by rotating a magnet. When the axis of rotation of the magnet was perpendicular to the substrate, the microparticles rotated around the same vertical axis but with a sense of rotation opposite to that of the magnet. Figure 2c shows a schematic depiction of this simple rotation as well as OM images of a rotating microparticle, taken at time intervals of 0.084 s (see Movie S2 in the Supporting Information). On the other hand, when the axis of rotation of the magnet was in the plane of the substrate, translation of the microparticles by a rolling motion was induced. In fact, except when the axis of rotation is perpendicular to the substrate, application of a rotating magnetic field causes the microspheres to roll on the substrate, as rotation and translation in a viscous medium are coupled owing to the presence of the substrate.[12] As we shall see below, the nanoscopic surface structure enhances the coupling intensity between rotation and translation owing to the increased hydrodynamic lubrication resistance. Figure 2d shows a magnetic particle undergoing translational motion, and Movie S2 in the Supporting Information shows this motion more explicitly. In this case, the direction of motion could be controlled by varying the direction of magnet rotation.

The translational velocity strongly depended on the rotational frequency of the magnet as well as on the size and surface roughness of the microparticles. To investigate the effect of these three factors, we performed experiments on magnetic particles prepared with and without silica particles. For the microparticles with silica particle arrays on their surfaces, we applied a magnetic field to the suspended droplets for 1 min prior to droplet solidification. Although 1 min is insufficient time to induce phase separation of the nanoparticles, it is sufficient to induce the alignment of the magnetic moment of the nanoparticles and thus to create a net magnetic moment within the individual microparticles. Movie S3 in the Supporting Information shows the motion of microparticles prepared with and without application of the magnetic field. The particles that were subjected to the magnetic field during synthesis exhibit vigorous translational motion, whereas the particles prepared without use of a magnetic field show only vibrational motion without translation. For the smooth magnetic particles lacking silica particles, we applied the magnetic field to the suspended droplets for 10 s. We found that when a rotating magnetic field whose axis of rotation is parallel to the substrate was applied to 173 μm diameter microparticles with smooth surfaces, the translational velocity increased with increasing frequency of magnet rotation (Figure 3a, red dotted line).

To examine the relative rates of translation and rotation, we plotted the ratio $v/\pi Df$ versus the frequency of the rotating field (f), where v and D denote the microparticle velocity and diameter, respectively. As can be seen from the blue dotted line in Figure 3a, the ratio decreases as the frequency increases, and it exceeds 0.25 across the entire range of frequencies used. Theoretically, this ratio is always close to 0.25 for a rotating sphere without external forces in the lubrication limit.[12] The enhancement of the ratio observed in our system is attributed to the external magnetic force on the particles that arises from the nonuniform magnetic field generated by the magnet, where the force is proportional to the gradient of the square of the magnetic field.[13] Under a

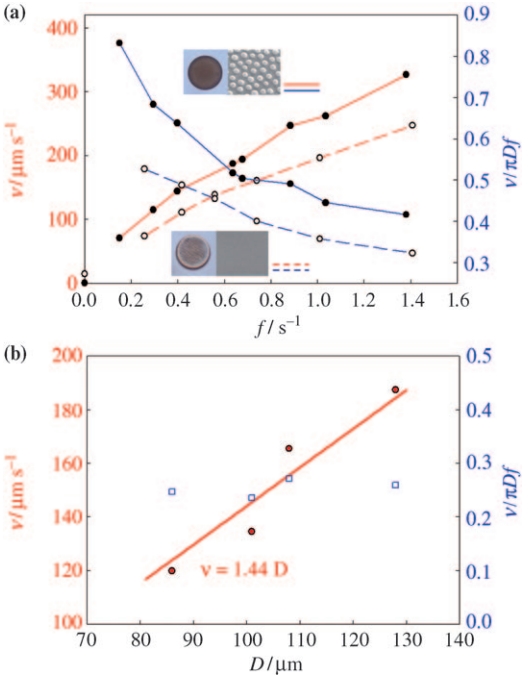

Figure 3. a) Graphs of translational velocity (red) and the relative rates of translation and rotation (blue) of magnetic particles with (●) and without (○) surface complexity under a rotating magnetic field. b) Size dependence of the translation velocity of magnetic particles; the frequency of magnet rotation was 1.8 s^{-1} in all cases.

static field, the magnetic particles show slow translation (14.5 μm s^{-1}, denoted by the empty circle at zero frequency), thus indicating that the magnet generates a nonuniform field and force on the particles. Because the effect of the force decreases as the frequency increases, the ratio decreases toward a value of 0.25. By comparison, for 181 μm diameter microparticles with silica particle arrays, the surface roughness enhanced the translational velocity. As a result, the ratio of the rates of translation and rotation was higher for these particles than for the particles with smooth surfaces (Figure 3a, blue solid line). It is noteworthy that the microparticles with silica particle arrays do not move under the static magnetic field (filled circle at zero frequency), although the particles did move slowly when the substrate was shaken side to side. These findings may be related to an increase in mechanical interference and solid–solid friction associated with the increase in nanoscale surface roughness of the microparticles.[12] Solid–solid friction can reduce the slip of microparticles on the substrate and thus increase the translational velocity.

The effect of microparticle size on velocity was straightforward to analyze. If the ratio of translation to rotation rate is independent of the particle size, the translational velocity is proportional to the microparticle diameter. Indeed, we observed a linear relationship between diameter and translational velocity for the frequency of 1.8 s^{-1} (Figure 3b). The average ratio of the translation to rotation rate is 0.254, as determined from the slope of the curve. Figure S3 in the Supporting Information shows how the different translational velocities of differently sized particles can be exploited to induce the spatial separation of a mixture of polydisperse microparticles by applying a magnetic field to induce translational motion. The translational motion of microparticles in the bulk is shown in Movie S4 in the Supporting Information.

Next, to demonstrate an application of the remote control of microparticle motion, we performed experiments in which we separated individual microparticles from a mixture of three types of particle: 1) untreated, 2) fluorescein isothiocyanate (FITC)-treated, and 3) tetramethyl rhodamine isothiocyanate (TRITC)-treated microparticles. The latter two types of microparticles were generated by treating the Janus particles with the relevant dye molecules. These treatments used a silane coupling agent to bind the dye molecules to the silanol groups on the exposed surfaces of the silica arrays. Note that biomolecules such as proteins can also be bound to the surfaces of the silica particles through simple chemistry (Figure S4 in the Supporting Information). To separate the mixture of untreated, FITC-treated, and TRITC-treated microparticles, the microparticle mixture was introduced into a microfluidic channel that split into three channels connected to three distinct chambers (Figure 4). The chambers were wells whose bases were lower than the level of the channel. In the microfluidic device, the motions of the microparticles are constrained by the channel walls and chambers, making it possible to control the movements of individual microparticles and hence to guide each microparticle into the desired chamber by application of a rotating magnetic field that has its axis parallel to the substrate. Figure 4a shows an OM image of the microfluidic device containing the microparticles. By comparing with the fluorescence microscope image (inset), we can identify the tag of each microparticle. In Figure 4, untreated, FITC-treated, and

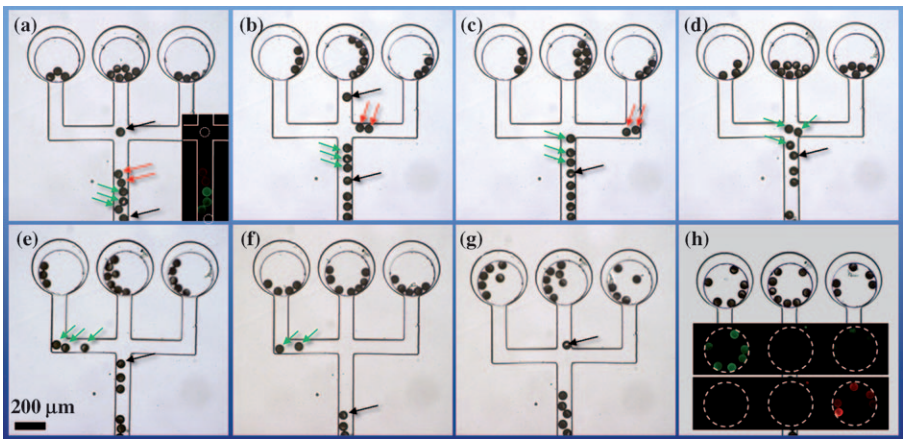

Figure 4. OM images displaying separation of magnetic Janus particles in a microfluidic device. Insets of (a) and (h) show fluorescent microscope images. The black, red, and green arrows denote the untreated, TRITC-treated, and FITC-treated magnetic Janus particles.

TRITC-treated microparticles are denoted with black, green, and red arrows, respectively. In the experiment, the aim was to guide these microparticles into the middle, left, and right chambers, respectively. Figure 4b shows the system at a point at which one black microparticle is advancing straight ahead while two red microparticles are moving in the right-hand channel. The magnetic field applied to move the red particles toward the right causes the black and green microparticles in the main channel to rest against the right wall of the channel. A short time later (Figure 4c), the black particle has reached the middle chamber, and the two red microparticles have arrived at the corner of the right-hand channel. Subsequently, we applied an upward motion to advance the two red microparticles into the right-hand chamber (Figure 4d). In a similar manner, we separated the three green and one black microparticle into the left and middle chambers (Figure 4e–h). By designing the chambers such that their bases are lower than the channel, we could impart backward motions to the microparticles in the channels without affecting the particles already in the chambers, which is occasionally needed in the separation procedure. The two fluorescence microscope images in the inset of Figure 4h demonstrate the successful separation of the microparticles.

In conclusion, we have prepared magnetic Janus microparticles with complex surface structures and have demonstrated the remote manipulation of these particles. The magnetic microparticles responded to an external magnetic field on a time scale of less than 0.1 s and exhibited rotational and translational motion under a rotating magnetic field. The translation velocity achieved under a rotating magnetic field was dramatically enhanced compared to that achieved by simple magnetophoretic movement in a static field. Furthermore, the complex surface structures afforded by the silica arrays enhanced the translational velocity. Notably, the silica arrays on the particle surfaces had the additional advantage that they have functional groups to which chemicals or biomolecules can be bound through simple chemistry. Our findings indicate that such magnetic Janus particles have great potential in a wide range of microparticle-based biological systems, including high-throughput immunoassays and biological probes as well as microfluidic pumps and mixers.[14]

Experimental Section

Preparation of the suspensions: Monodisperse silica particles of diameter 330 nm were synthesized using the Stöber method.[15] The silica powders and iron oxide (α-Fe_2O_3) nanoparticles (smaller than 50 nm, Aldrich) were dispersed in ethanol and mixed with ETPTA resin (Aldrich) containing photoinitiator (Irgacure2100, Ciba Specialty Chemicals). The amounts of silica particles and iron oxide nanoparticles were chosen such that their weight fractions in the final, ethanol-free ETPTA were 10% and 0.2%, respectively. After complete mixing, ethanol was selectively evaporated for 12 h (at 70 °C), and the silica and iron oxide nanoparticle-in-ETPTA suspension was sonicated for 30 min.

Preparation of monodisperse droplets and phase separation: To prepare monodisperse droplets of the photocurable suspension, we used a microfluidic glass capillary device composed of two coaxial capillaries. The photocurable suspension was introduced into the inner capillary, and an aqueous solution of 1 wt% Pluronic F108 (ethylene oxide–propylene oxide–ethylene oxide triblock copolymer surfactant; BASF) was introduced through the outer capillary. To achieve stable generation of emulsion droplets in the dripping regime, the flow rate of the suspension was controlled such that it was lower than that of the aqueous solution. The monodisperse droplets were collected in a glass Petri dish from the end of the outer capillary. To induce the alignment and magnetophoretic movement of iron oxide nanoparticles within the droplets, the glass Petri dish was sandwiched between two disc-type magnets for 30 min. After phase separation, the magnets were removed and UV irradiation from a mercury lamp was applied to the Petri dish for 2 s to solidify the droplets into microparticles.

Movement control of magnetic Janus microparticles: The poly(dimethylsiloxane) (PDMS) microfluidic device was prepared using a conventional soft-lithographic technique, by which the photoresist pattern was fabricated by two steps of UV exposure with two different photomasks to create chambers that were deeper (250 μm) than the channels (150 μm). To fill the chambers with ethanol, we introduced ethanol into the channels leading to the chambers under pressure for 5 h; during this time, the air in the chambers diffused out through the PDMS, leaving the chambers filled with ethanol. The magnetic Janus particles dispersed in ethanol were introduced at the entrance of the channel and moved into the channel and chamber when a rotating magnetic field was applied that was generated by rotating a magnet of 3.35 kG on the surface at a distance of approximately 7 cm from the magnetic particles.

Received: February 19, 2010
Published online: April 14, 2010

Keywords: colloids · magnetic properties · microfluidics · rotation · translation

[1] a) M. Han, X. Gao, J. Z. Su, S. Nie, *Nat. Biotechnol.* **2001**, *19*, 631; b) J.-M. Nam, C. S. Thaxton, C. A. Mirkin, *Science* **2003**, *301*, 1884.

[2] F. Wurm, A. F. M. Kilbinger, *Angew. Chem.* **2009**, *121*, 8564; *Angew. Chem. Int. Ed.* **2009**, *48*, 8412.

[3] a) S. Xu, Z. Nie, M. Seo, P. Lewis, E. Kumacheva, H. A. Stone, P. Garstecki, D. B. Weibel, I. Gitlin, G. M. Whitesides, *Angew. Chem.* **2005**, *117*, 3865; *Angew. Chem. Int. Ed.* **2005**, *44*, 3799; b) D. Dendukuri, K. Tsoi, T. A. Hatton, P. S. Doyle, *Langmuir* **2005**, *21*, 2113; c) D. K. Hwang, D. Dendukuri, P. S. Doyle, *Lab Chip* **2008**, *8*, 1640; d) S.-H. Kim, S.-J. Jeon, G.-R. Yi, C.-J. Heo, J. H. Choi, S.-M. Yang, *Adv. Mater.* **2008**, *20*, 1649.

[4] a) Z. Nie, W. Li, M. Seo, S. Xu, E. Kumacheva, *J. Am. Chem. Soc.* **2006**, *128*, 9408; b) R. F. Shepherd, J. C. Conrad, S. K. Rhodes, D. R. Link, M. Marquez, D. A. Weitz, J. A. Lewis, *Langmuir* **2006**, *22*, 8618; c) T. Nisisako, T. Torii, T. Takahashi, Y. Takizawa, *Adv. Mater.* **2006**, *18*, 1152; d) S.-H. Kim, S.-J. Jeon, W. C. Jeong, H. S. Park, S.-M. Yang, *Adv. Mater.* **2008**, *20*, 4129; e) K. P. Yuet, D. K. Hwang, R. Haghgooie, P. S. Doyle, *Langmuir*, **2010**, *26*, 4281.

[5] a) Z. Nie, S. Xu, M. Seo, P. C. Lewis, E. Kumacheva, *J. Am. Chem. Soc.* **2005**, *127*, 8058; b) J.-W. Kim, A. S. Utada, A. Fernandez-Nieves, N. Hu, Z. Hu, D. A. Weitz, *Angew. Chem.* **2007**, *119*, 1851; *Angew. Chem. Int. Ed.* **2007**, *46*, 1819; c) S.-H. Kim, S.-J. Jeon, S.-M. Yang, *J. Am. Chem. Soc.* **2008**, *130*, 6040; d) C.-H. Chen, A. R. Abate, D. Lee, E. M. Terentjev, D. A. Weitz, *Adv. Mater.* **2009**, *21*, 3201.

[6] a) D. Dendukuri, D. C. Pregibon, J. Collins, T. A. Hatton, P. S. Doyle, *Nat. Mater.* **2006**, *5*, 365; b) D. C. Pregibon, M. Toner, P. S. Doyle, *Science* **2007**, *315*, 1393.

[7] a) S. E. Chung, W. Park, H. Park, K. Yu, N. Park, S. Kwon, *Appl. Phys. Lett.* **2007**, *91*, 041106; b) S. E. Chung, W. Park, S. Shin, S. A. Lee, S. Kwon, *Nat. Mater.* **2008**, *7*, 581.

[8] R. M. Erb, N. J. Jenness, R. L. Clark, B. B. Yellen, *Adv. Mater.* **2009**, *21*, 4825.
[9] S.-H. Kim, S. Y. Lee, S.-M. Yang, *Angew. Chem.* **2010**, *122*, 2589; *Angew. Chem. Int. Ed.* **2010**, *49*, 2535.
[10] R. M. Cornell, U. Schwertmann, *The Iron Oxides*, VCH, Weinheim, **1996**, chap. 6.
[11] a) B. P. Binks, S. O. Lumsdon, *Langmuir* **2000**, *16*, 8622; b) L. Hong, S. Jiang, S. Granick, *Langmuir* **2006**, *22*, 9495; c) S.-H. Kim, C.-J. Heo, S. Y. Lee, G.-R. Yi, S.-M. Yang, *Chem. Mater.* **2007**, *19*, 4751; d) S.-H. Kim, J. W. Shim, J.-M. Lim, S. Y. Lee, S.-M. Yang, *New J. Phys.* **2009**, *11*, 075014.
[12] A. J. Goldman, R. G. Cox, H. Brenner, *Chem. Eng. Sci.* **1967**, *22*, 637.
[13] H. Bruus, *Theoretical Microfluidics*, Oxford University Press, New York, **2008**, chap. 10.
[14] J. Leach, H. Mushfique, R. di Leonardo, M. Padgett, J. Cooper, *Lab Chip* **2006**, *6*, 735.
[15] W. Stober, A. Fink, E. Bohn, *J. Colloid Interface Sci.* **1968**, *26*, 62.

